Influence of Differently Ionized Species on Fragmentation Pathways and Energetics of a Potential Adenosine Receptor Antagonist Using a Triple Quadrupole and a Multistage LTQ-Orbitrap™ FTMS Instrument

Wendy Zhong,* Patrick A. Irish, and Gary E. Martin

Rapid Structure Characterization Laboratory Pharmaceutical Science, Schering-Plough Research Institute, Summit, New Jersey 07901
*E-mail: wendy.zhong@spcorp.com

Received August 21, 2008
DOI 10.1002/jhet.196
Published online 25 June 2009 in Wiley InterScience (www.interscience.wiley.com).

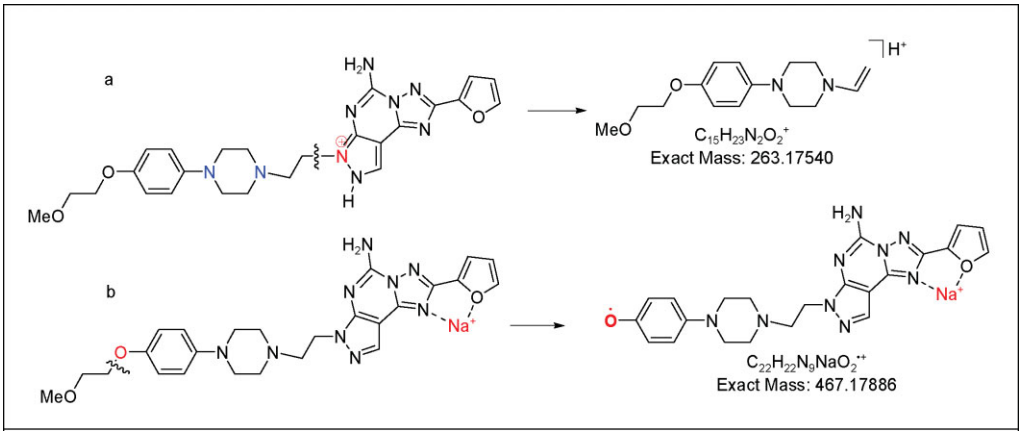

A systematic study was conducted to investigate the influence of differently ionized species on the fragmentation pathways and energetics of a piperazine-containing adenosine by using different cations or anions. Very different fragmentation mechanisms were observed in protonated- *versus* sodiated-molecules, which indicated that the proton is mobilized to promote the charge-direct fragmentation, whereas Na^+ cation was fixed at the heterotricyclic ring structure provoking charge-remote fragment ions. This finding was also supported by the results observed in the fragmentation behaviors in the deprotonated-molecule. The energetics of these fragment ions were also explored by using the breakdown curves obtained from the triple quadrupole and LTQ-Orbitrap™ instrument. The data indicated that the lowest energy pathways in the protonated-molecule $[M+H]^+$ involve breaking a C—N bond connecting an ethylene bridge and heterotricyclic ring structure. The lowest energy pathway is the cleavage of a C—O bond connecting the methoxy ethyl group and phenolic oxygen to form a distonic radical ion for a sodiated-molecule $[M+Na^+]$and a deprotonated-molecule $[M-H]^-$. The data suggest that by choosing the differently ionized species, one can probe different fragmentation channels that can provide additional structure information for an unknown impurity and possibly degradation product identification. In addition, by comparing the data obtained from triple quadrupole and LTQ-Orbitrap instruments, one can develop further understanding of the differences in the fragmentation behaviors due to the variations in the collision activation-dissociation process. From the side-by-side comparison with the breakdown curves obtained for both instruments, the difference in fragmentation behaviors caused by the difference in dissociation processes that occur in these two types of instruments can be probed.

J. Heterocyclic Chem., **46**, 591 (2009).

INTRODUCTION

LC/MS and LC/MS/MS techniques have become a widely used analytical tool for the identification of small molecule impurities in active pharmaceutical ingredients (API). With the increasing number of applications of LC/MS and MS/MS methods, a comprehensive understanding of small-molecule fragmentation pathways has become correspondingly more important. The newly designed LTQ-Orbitrap™ instrument has the capability of performing high-resolution (upto 100,000) and high-mass accuracy (<5 ppm, external calibration) with wide-dynamic range (>5000) mass measurements [1,2]. The instrument can also perform multistage MS/MS (MS^n) experiment that are essential for studying fragmentation pathways.

A potential adenosine receptor antagonist, **1**, was utilized as a model compound for this mass spectral fragmentation pathway study.

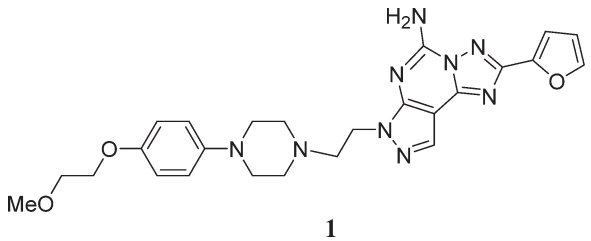

1

The fragmentation mechanisms and energetics of these types of compounds have not been explored previously. To identify potential impurities and degradation products in **1**, and related compounds, it is essential to understand the fragmentation pathways and energetics of this model compound. The LTQ-Orbitrap is a hybrid instrument that combines an LTQ ion trap instrument with an Orbitrap; the latter is used for high-mass accuracy analysis. All the ion activation processes occur in the LTQ ion trap portion of the instrument, and the resulting ions are then injected into the Orbitrap to achieve high-mass accuracy detection. In an ion trap, collisonal-activation of the precursor ion occurs *via* resonance excitation that couples with the tandem-in-time process of the ion trap, rather than tandem-in-space process of a beam instrument. This allows multistage tandem mass spectrometry for structural elucidation. Combining multistage MS/MS experiments with high-resolution detection obtained in the Orbitrap, one can obtain high-mass accuracy (<5 ppm) for every fragment ion. Consequently, we are able to determine the elemental composition of each fragment ion, allowing the derivation of plausible fragment structures. As a result, a detailed fragmentation pathway of a compound can be readily derived *via* these experiments. Themo Fisher Quantum triple quadrupole mass spectrometer is a beam instrument where collision activation of precursor ions occurs through tandem-in-space was used for comparison purposes [3,4]. The differences in fragmentation behavior of the model compound were illustrated clearly from the breakdown curves generated by both instruments.

In this article, we discuss the influence of the different cations or anions on the fragmentation behavior of **1**, especially, the protonated, sodiated, and deprotonated adducts commonly observed in a routine LC/MS run. The different fragmentation behaviors observed from these varied approaches can assist the investigator in determining additional fragmentation channels that are structurally informative. By applying different approaches, the process can help an investigator to interpret the fragmentation patterns generated in unknown impurities and degradation products leading ultimately to the determination of the structure. Charge-remote fragmentation mechanism of the sodium adduct were also studied. The purpose was to provoke the charge-remote fragmentation by using the Na^+ cation instead of the protonated-molecule to gain access to different types of fragmentation channels. A similar approach has been successfully applied to other types of compounds previously [5,6].

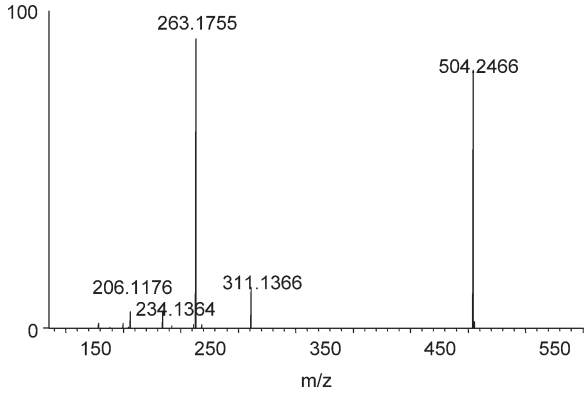

Figure 1. 30 eV MS/MS spectrum of the protonated-molecule at m/z 504 obtained from Orbitrap MS.

RESULTS AND DISCUSSION1

Protonated-molecule. Figure 1 shows the 30 eV MS/MS spectrum of the protonated-molecule, 1, at m/z 504, obtained from the Orbitrap instrument. The most abundant fragment ion at m/z 263 was the result of the cleavage C—N bond with a neutral loss of 7*H*-pyrazolo[4,3-*e*]-[1,2,4]triazolo-[1,5-*c*]pyrimidin-5-yl amine moiety (a heterotricyclic moiety, see Scheme 1). The fragment ion at m/z 311 was the result of piperazine ring opening with a neutral loss of the methoxy-phenetole and a portion of the piperazine ring. MS^3 experiments were also conducted to further investigate the fragmentation pathway of this compound. Figure 2 shows the MS^3 spectra of the product ions at m/z 263 and m/z 311. As shown in Scheme 1, the fragment ion at m/z 263 yields two dominant fragment ions at m/z 206 generated by piperazine ring opening and 234 produced by the loss of the ethylene bridge. The fragment ion at m/z 206 undergoes further fragmentation to give an ion at m/z 178. The fragment ion at m/z 311 gave two major fragment ions at m/z 268 (the result of loss of a vinyl amine group) and 242 generated by cleavage at the C—N bond between the carbon of the ethylene linkage and the nitrogen on the tricyclic ring. The data show that all the fragment ions were the result of either the piperazine ring opening or the cleavage at either side of the ethylene linkage connecting the phenyl piperazine and hetero tricyclic moieties.

For comparison purposes, the 30 eV MS/MS spectrum of the protonated-molecule (m/z 504) generated by a

Scheme 1. Fragmentation pathways of the protonated-molecule at m/z 504 derived from MS^3 spectra obtained from the Orbitrap instrument at mass accuracy within 1 ppm. [Color scheme can be viewed in the online issue, which is available at www.interscience.wiley.com.]

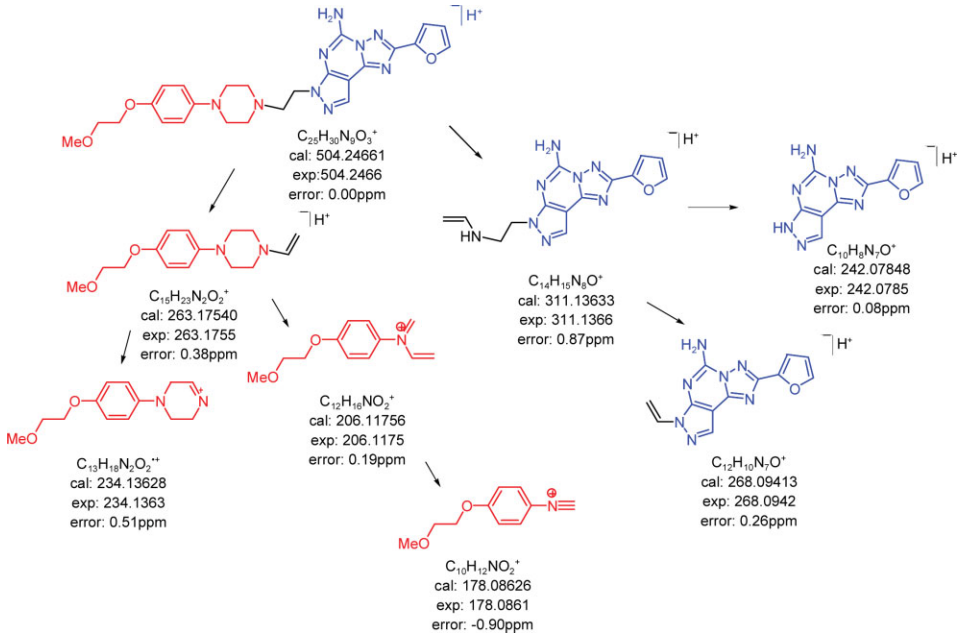

triple quadrupole instrument is shown in Figure 3. The fragmentation patterns were similar to those obtained from the Orbitrap instrument except for the differences in the relative abundances of individual fragment ions. The MS/MS data suggested that preferential and selective cleavage was observed in the protonated-molecule obtained *via* the Orbitrap instrument, whereas extensive and nonselective cleavage was generated by the triple quadrupole instrument.

To illustrate energy effects on the fragmentation behavior more clearly, the breakdown curves obtained from both Orbitrap and triple quadrupole instruments are shown in Figure 4. It is clear that the breakdown curve obtained from the Orbitrap instrument changes dramatically with changing the collision energy from 20 to 35 eV. The intensity for the precursor ion decreases with increasing collision energy. At 35 eV collision energy, almost all the precursor ions underwent further fragmentation, the fragment ion at m/z 263 becoming the most dominant peak. The relative intensity of each fragment ion remained unchanged when the collision energy was increased from 35 to 60 eV. The major fragment ion at m/z 263 remained the dominant fragment ion, whereas all the other fragment ions were present at very low intensity. The data indicated that the m/z 263 ion was the low energy and preferred fragmentation channel. The collision activation dissociation process occurred in a linear ion trap, where the ion of interest collided multiple times with helium gas but could not accumulate enough internal energy to facilitate the higher energy fragmentation channels.

The breakdown curves obtained from the triple quadrupole instrument changed dramatically *via* changes of the collision energy as shown in Figure 4(b). The collision energy had a significant impact on the fragmentation channels. The precursor ion intensity decreases with the increase of the collision energy from 0 to 40 eV. Above 40 eV, the precursor ion intensity was less than 5%. Concurrently, the fragment ion intensity increased dramatically. At around 30 eV, the fragment ion at m/z 263 became the dominant fragmentation channel, which is consistent with the observation from Orbitrap instrument, where the m/z 263 is the lowest energy channel in the protonated-molecule. When the collision energy increased to around 40 eV, the fragment ions at m/z 84 and 206 became the dominant fragmentation channels. When the collision energy was increased to 50 eV, m/z 178 became the major fragment channel.

Based on the Scheme 1, it is clear that the fragment ions at m/z 84, 178, and 206 were the result of further dissociation of the fragment ion at m/z 263. The data suggest that in the triple quadrupole instrument, there is enough internal energy deposited into the molecule to promote higher energy fragmentation channels.

The breakdown curves obtained from both instruments also demonstrated that the dominant fragment ions, such as, m/z 263, 206, 178, and 84 contained the whole or partial piperazine ring. The fragment ions containing the 7*H*-pyrazolo[4,3-*e*][1,2,4]-triazolo[1,5-*c*]pyrimidin-5-yl amine, such as m/z 311, 268, and 242, were present in a very small amount. It is clear that in the

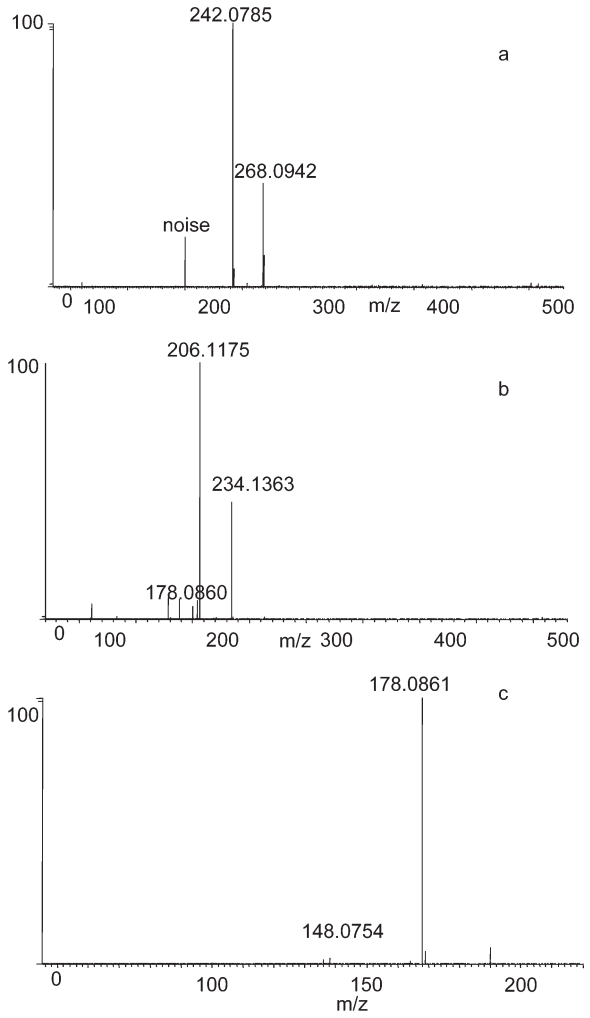

Figure 2. (a) 30 eV MS^3 spectrum of the protonated-molecule at m/z 504→m/z 311→ product, (b) 35 eV MS^3 spectrum of the protonated-molecule at m/z 504→m/z 263→ product, and (c) 30 eV MS^3 spectrum of the protonated-molecule at m/z 504→m/z 206→ product.

protonated-molecule, **1**, the preferred fragmentation channels involved the phenyl piperazine moiety.

Sodiated-molecule[M+Na^+]. Figure 5(a) shows the 20 eV MS/MS spectrum of the sodiated-molecule at m/z 526 in the Orbitrap MS instrument. Again, very selective and preferential cleavage was observed in the sodiated-molecule in the Orbitrap instrument. Only one fragment ion at m/z 467 was observed at collision energies ranging from 0 to 70 eV in the Orbitrap instrument. Based on the accurate mass data, the structure of this fragment ion can be determined as a nonconventional distonic radical cation (Scheme 2). This fragment ion was not observed for the protonated-molecule (Fig. 1 and Scheme 1). To explore the fragmentation behaviors of the sodiated-molecule, MS^3 experiments of the product ion at m/z 467 generated from the sodiated-molecule at m/z 526 were conducted [Fig. 5(b)]. The major fragment ions observed were m/z 333, 319, 290, and 264, in which, m/z 333, 290, and 264 correspond to fragment ions at m/z 311, 268, and 242 in the protonated-molecule. The fragment ion at m/z 319, the most dominant fragment in the 30 eV MS^3 spectrum using the Orbitrap MS, was not present for the protonated-molecule. This fragment ion was the result of piperazine ring opening in a different way from that of the m/z 333 ion. The fragmentation pathways derived from the MS/MS and

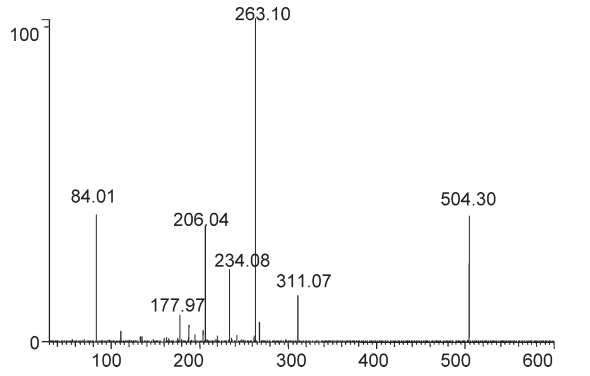

Figure 3. 30 eV MS/MS spectrum of the protonated-molecule at m/z 504 obtained from triple quadrupole instrument.

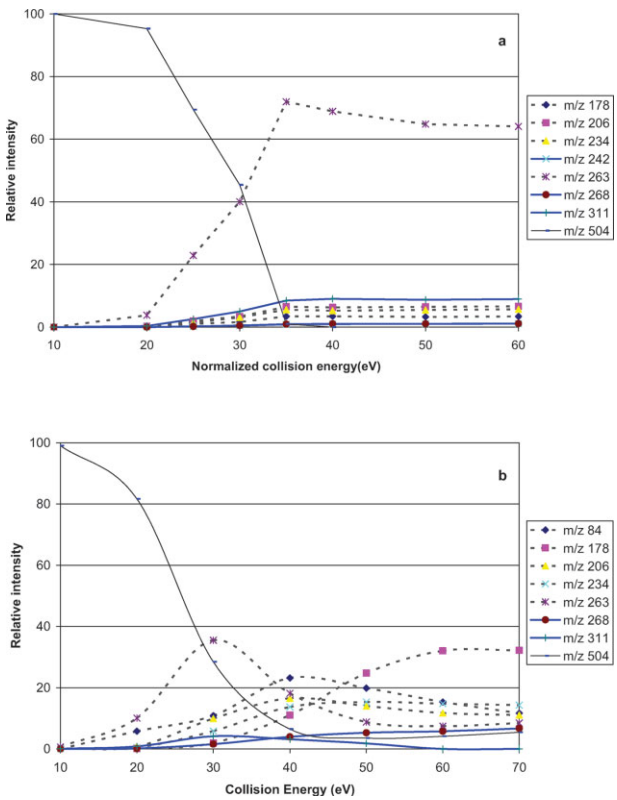

Figure 4. (a) Breakdown curve of $[M+H]^+$ from Orbitrap; (b) Breakdown curve of $[M+H]^+$ from triple quadrupole. [Color figure can be viewed in the online issue, which is available at www.interscience.wiley.com.]

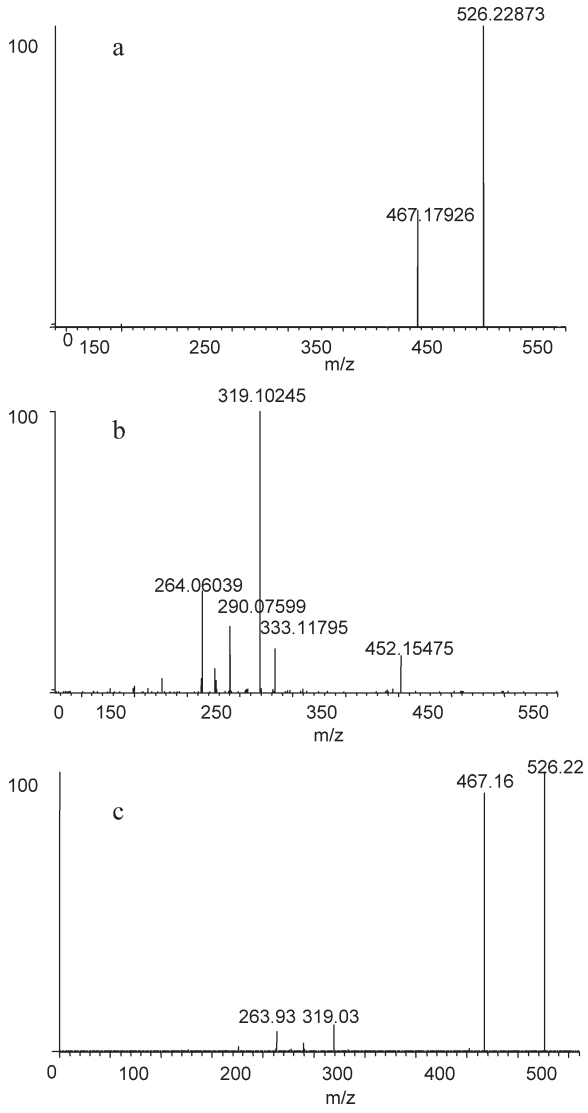

Figure 5. (a) 20 eV MS/MS spectra of $[M+Na^+]$ at m/z 526 from the Orbitrap MS, (b) 35 eV MS^3 spectrum of $[M+Na^+]$ at m/z 526→ m/z 467→products from the Orbitrap MS, (c) 30 eV MS/MS of $[M+Na^+]$ at m/z 526 from the triple quadruple MS.

MS^3 experiments in the Orbitrap MS instrument are depicted in Scheme 2. It is worth noting that contrary to the fragmentation patterns observed for the protoned-molecule the major fragment ions in the MS^3 spectrum of the sodiated-molecule from the Orbitrap instrument all contain the intact 7*H*-pyrazolo[4,3-*e*][1,2,4]triazolo[1,5-*c*]pyrimidin-5-yl amine tricyclic ring moiety.

Figure 5(c) shows the 30 eV MS/MS spectrum of $[M+Na^+]$ generated by a triple quadrupole instrument at 30 eV collision energy. The data showed the dominant fragment ion was observed at m/z 467, which is consistent with that obtained from Orbitrap instrument. However, in a triple quadrupole, we also observed several fragment ions at m/z 226, 264, 290, and 319, which were absent from the MS/MS spectrum generated in an Orbitrap instrument. Interestingly, all these ions were only observed in a MS^3 spectrum of the product ion at m/z 467 using the Orbitrap instrument.

Figure 6(a,b) shows the breakdown curves generated by the Orbitrap and triple quadrupole instruments. The breakdown curves generated by the Orbitrap were very simple. Only one fragment ion at m/z 467 was generated at collision energy ranging from 0 to 80 eV with He as the collision gas. The data demonstrated that only one fragmentation channel opened during MS/MS experiment in Orbitrap and that forming the fragment ion at m/z 467 was the lowest energy process.

Figure 6(b) exhibits very interesting and different breakdown curves generated by the triple quadrupole instrument. Overall, the fragmentation behavior changed dramatically with increasing collision energy. At lower energy, the precursor ion intensity decreased with increasing collision energy. Only 50% of the precursor ion remained at collision energy of 30 eV; the dominant fragment ion observed at this collision energy was m/z 467, which indicated that this is the lowest energy channel. Many fragmentation channels were opened up when the fragment ion at m/z 319 became the major fragment ion at 40–50 eV collision energy. At a collision energy of 60 eV, the m/z 264 fragment ion was the most favored. The data clearly suggest that there were more internal energy deposited in the dissociation process in a triple quadrupole instrument, which opens up higher energy fragmentation channels.

The remarkable differences between breakdown curves obtained from the Orbitrap and triple quadrupole instruments for protonated- and sodiated-forms of **1** are the relative abundance of fragment ions at m/z 263 (protonated) and m/z 467 (sodiated). These differences are most likely caused by discrimination against certain fragment ions in competitive reaction channels in slow activation processes common in ion trap instruments [8,9]. Based on the study conducted by Futrell and coworkers [8], two different fragmentation pathways are competing with each other: the further dissociation of the lowest-energy fragmentation *via* high-energy fragmentation channel. The higher energy fragmentation pathway is strongly suppressed if it has a slower-activation process than that of the low-energy pathway(s). These observations were also consistent with the results of other ion-activation processes, such as surface-induced dissociation (SID) *vs*. collision induced dissociation (CID) reported by Laskin *et al*. [10]

We also wished to compare the fragmentation pathways obtained using the Orbitrap instrument (Schemes 1 and 2) and breakdown curves generated by triple quadrupole instrument [Figs. 4(b) and 6(b)] for both protonated- and sodiated-molecule, respectively. It is clear that all the dominant fragment ions in the protonated-

Scheme 2. Fragmentation pathways of [M+Na$^+$] from Orbitrap instrument with mass accuracy of 1 ppm. [Color scheme can be viewed in the online issue, which is available at www.interscience.wiley.com.]

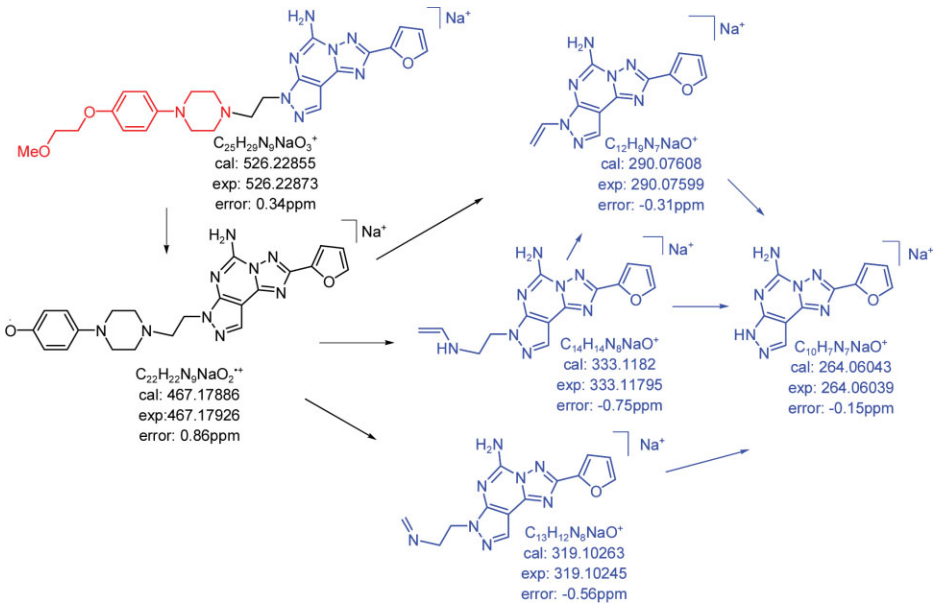

molecules contain the piperazine moiety, whereas the major fragment ions in the sodiated-molecules contain a heterotricyclic moiety. The data may be explained by the proposed fragmentation mechanism shown in Scheme 3. In the protonated-molecule, the proton is freely mobilized in the molecule, which will promote charge-directed fragmentation. For example, when the proton is on a nitrogen atom of the tricyclic ring, it will weaken the C—N bond, which breaks to form the dominant fragment ion at m/z 263. The mobile proton model was also applied to explain the fragmentation behavior for protonated-peptides [11]. Conversely, for the sodiated-molecule, sodium cation is localized at the heterotricyclic moiety, which can provoke charge-remote fragment ions [12–14]. For example, the dominant fragment ion at m/z 467 was obtained through homolytic cleavage of a C—O bond to form the distonic radical cation, with 0.11 ppm mass accuracy. The data from deprotonated-negative ion [M-H]$^-$, as described in the next section, further supported this hypothesis.

Deprotonated-negative ion [M-H]$^-$. Figure 7(a,c) show the 30 eV MS/MS spectra of the deprotonated-molecule at m/z 502 obtained by Orbitrap and triple quadrupole instruments. Similar fragmentation patterns were observed in both instruments, with the major fragment ion at m/z 443, which is speculated to be a distonic radical ion formed *via* the breaking C—O bond, corresponding to m/z 467 ion in sodiated-molecule. Figure 7(b) shows the 35 eV MS^3 spectrum of the product ion at m/z 443, the major fragment ion from the precursor ion at m/z 502. The major fragment ions at m/z 295 and 252 were generated by the piperazine ring opening and C—C breaking in the ethylene moiety. The fragmentation pathways of the deprotonated-negative ion at m/z 502 are presented in Scheme 4. It is worth noting that

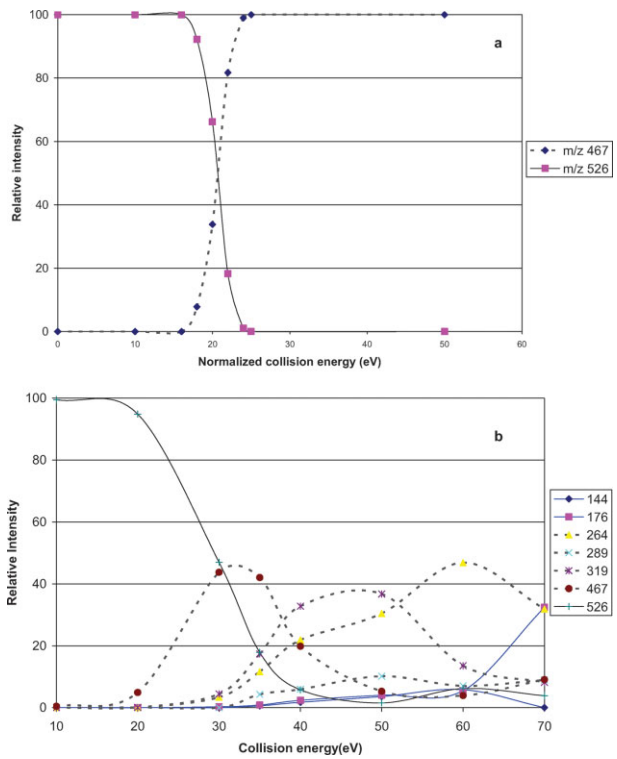

Figure 6. (a) Breakdown curve of [M+Na$^+$] from Orbitrap; (b) breakdown curve of [M+Na$^+$] from triple quadrupole. [Color figure can be viewed in the online issue, which is available at www.interscience.wiley.com.]

Scheme 3. The proposed fragmentation mechanism diagram: (a) $[M+H]^+$: mobile proton-charge direct fragmentation; (b) $[M+Na^+]$: fixed charge–charge remote fragmentation. [Color scheme can be viewed in the online issue, which is available at www.interscience.wiley.com.]

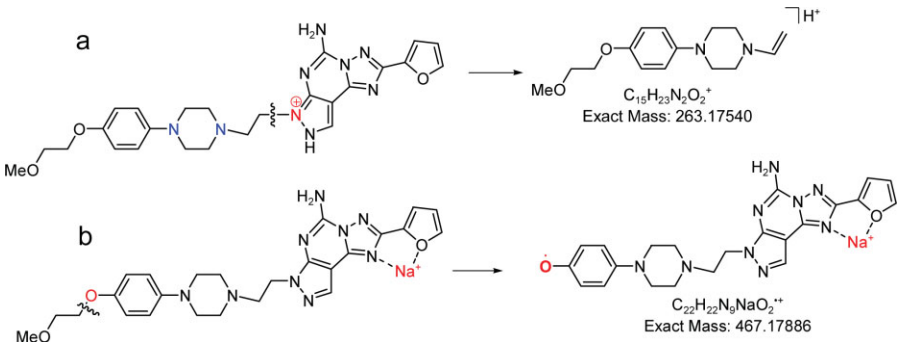

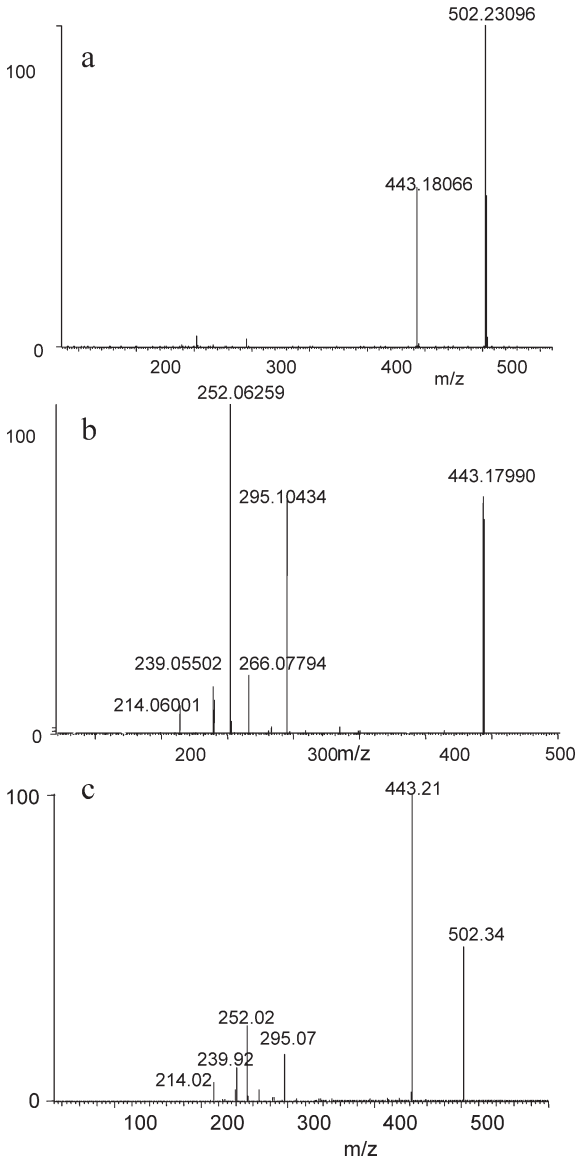

Figure 7. (a) 30 eV MS/MS spectra of $[M-H]^-$ from Orbitrap, (b) 35 eV MS^3 spectrum from Orbitrap, (c) 30 eV MS/MS spectra from triple quadrupole.

all the fragment ions from both MS/MS and MS^3 spectra contained a heterotricyclic moiety, which is similar to the behavior of the sodiated-molecule. The data suggest that the negative charge was located on the heterotricyclic moiety and all the fragment ions were again generated *via* charge-remote fragmentation mechanisms. This observation explains why the fragmentation patterns obtained from the deprotonated-molecule are similar to those obtained from the sodiated-molecule. A plausible hypothesis is that the only protons that can be removed in this molecule were those of the amino group connected to the tricyclic ring moiety, and the anion is localized/stabilized by the heterotricyclic ring moiety,

Scheme 4. Fragmentation pathways of $[M-H]^-$ from Orbitrap instrument. [Color scheme can be viewed in the online issue, which is available at www.interscience.wiley.com.]

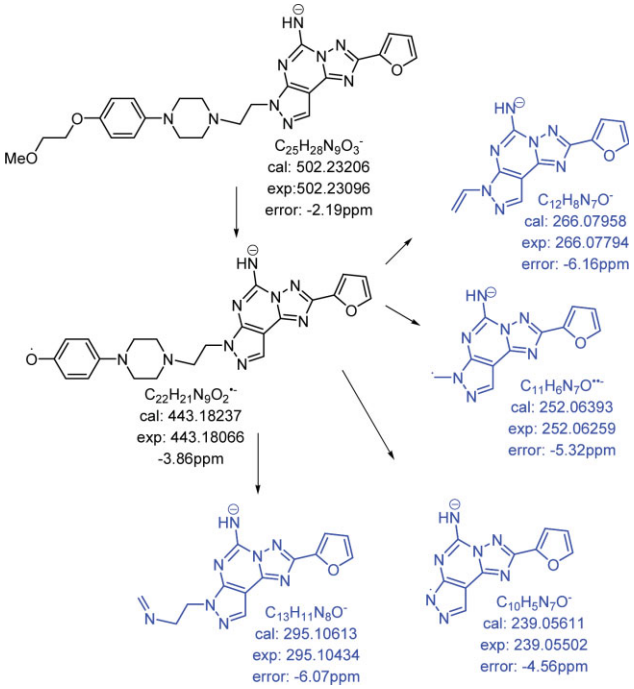

which promotes the charge-remote fragment ions as seen in the sodiated-molecule. The data served to further confirm that the fragmentation mechanisms for protonated-molecule and sodiated-molecule are different. Fragment ions generated in protonated-molecules were through charge-direct fragmentation, whereas the fragment ions generated in sodiated-molecules were *via* charge-remote fragmentation.

CONCLUSIONS

Fragmentation patterns differed substantially for the protonated- and sodiated–molecules, whereas the fragmentation patterns between the sodiated- and deprotonated-molecules were similar, with all the dominant fragmentation ions containing the hetero tricyclic moiety. The data suggest that the proton is mobile in a protonated-molecule to produce the charge-direct fragment ions, whereas the sodiated- or deprotonated-ions were localized/stabilized in the heterotricyclic moiety, to promote the formation of charge-remote fragment ions.

Based on the differences in the breakdown curves generated for the triple quadrupole and Orbitrap instruments, it is clear that higher internal energy was deposited into the molecule in the triple quadrupole instrument, whereas less internal energy was deposited in the Orbitrap instrument. The lowest energy fragmentation channel for the protonated-molecule was the formation of the fragment ion at m/z 263 formed *via* the cleavage between C—N bond connecting an ethylene linkage and heterotricyclic moiety. The lowest energy fragmentation channel for the sodiated- and deprotonated-molecule was the formation of the fragment ion at m/z 467 or 443 due to the cleavage of the phenole ether linkage. The data suggest that the preferential and selective cleavages at C—N and C—O in the protonated, deprotonated, and sodiated are likely to be observed in other adenosine receptor antagonist related compounds. These characteristic fragmentation patterns observed in Orbitrap MS/MS spectra will provide additional evidence in solving the unknown impurities related to adenosine receptor antagonist compounds. By fragmenting differently ionized species adducts, one can get additional fragmentation information helpful in pinpointing the location of the oxidation or chemical modification sites in the unknown molecules. Combining the fragmentation information obtained in both ion trap and triple quadrupole instrument, one can derive a more comprehensive understanding of the molecular structure and its behavior.

EXPERIMENTAL

Ion trap experiments. Experiments were conducted using a Thermo LTQ-Orbitrap instrument equipped with a Surveyor HPLC system. The high resolution LC/MS and LC/MS^n spectra were acquired in the FTMS mode of the Orbitrap instrument at 30,000 mass resolution and 5 ppm mass accuracy to obtain the elemental composition of each fragment ion. The electrospray ionization needle was held at 4.5 kV, and a nitrogen sheath gas (10 units), and a nitrogen auxiliary gas (20 units) were used to stabilize the spray. The heated-capillary was set at 270°C. All MS/MS experiments were conducted in the linear ion trap. Helium was introduced into the ion trap to improve the trapping efficiency and also serves as the collision gas for CID. Consequently, only helium can be used as collision gas with the Orbitrap instrument. The operational pressure after introducing helium was $\sim 2 \times 10^{-5}$ Pa in the linear ion trap.

Triple quadrupole experiments. The experiments were conducted in a Thermo Quantum triple quadrupole mass spectrometer equipped with a Surveyor HPLC system. Argon was used as collision gas at 0.1 Torr in all MS/MS experiments. The electrospray ionization needle was held at 4 kV, and a nitrogen sheath gas (10 units) and a nitrogen auxiliary gas (20 units) were used to stabilize the spray. The heated-capillary was set at 270°C.

About 1 mg/mL of adenosine receptor antagonist (**1**), which was synthesized and well characterized previously [7], was dissolved in 50:50 acetonitrile: water. Sample solutions were introduced to the mass spectrometer through the LC system. The protonated, sodiated, and deprotonated-molecule were formed during the LC run without introducing additional Na cation.

Acknowledgments. The authors thank Dr. Birendra Pramanik (Schering-Plough) and Dr. Michael Gross (Washington University) for their valuable discussion and comments.

REFERENCES AND NOTES

[1] Hardman, M.; Makarov, A. A. Anal Chem 2003, 75, 1699.
[2] Makarov, A.; Denisov, E.; Lange, O. J Am Soc Mass Spectrom 2006, 17, 977.
[3] Louris, J. N.; Cooks, R. G.; Syka, J. E. P.; Kelley, P. E.; Stafford, G. C., Jr.; Todd, J. F. Anal Chem 1987, 59, 1677.
[4] Johnson, J. V.; Yost, R. A.; Kelley, P. E.; Bradford, D. C.; Anal Chem 1990, 62, 2162.
[5] Chen, G.; Pramanik, B. N.; Bartner, P. L.; Saksena, A. K. J Am Soc Mass Spectrom 2002, 13, 1313.
[6] Cerny, R. L.; MacMillan, D. K.; Gross, M. L.; Mallams, A. K.; Pramanik, B. N. J Am Soc Mass Spectrom 1994, 5, 151.
[7] Kuo, S.; Tsai, D. J.; Tran, L. T.; Zhang, P.; Jones, A. D. U.S. Pat. Appl. Publ. CODEN: USXXCO US 2,005,090,492 A1 20,050,428 CAN 142:430,285 AN 2005:371,021 (2005), 15 pp.
[8] Laskin, J.; Denisov, E.; Futrell, J. J Phys Chem B 2001, 5, 1895.
[9] Laskin, J.; Futrell, J. H. Mass Spectrom Rev 2003, 22, 158.
[10] Laskin, J.; Yang, Z.; Lam, C.; Chu, I. K. Anal Chem 2007, 79, 6607.
[11] Dongre, A. R.; Jones, J. L.; Somogyi, A.; Wysocki, V. H. J Am Chem Soc 1996, 118, 8365.
[12] Adams, J. Mass Spectrom Rev 1990, 9, 141.
[13] Gross, M. L. Int J Mass Spectrom Ion Process 1992, 137, 118.
[14] Cheng, C.; Gross, M. L. Mass Spectrom Rev 2000, 19, 398.